

32. Correction of the operating modes of an induction motor with asymmetrical stator windings at vector control / Zagirnyak M., Kalinov A., Melnykov V., Kochurov I. // 2015 International Conference on Electrical Drives and Power Electronics (EDPE). 2015. doi: 10.1109/edpe.2015.7325303
33. Zagirnyak M., Maliakova M., Kalinov A. Analysis of operation of power components compensation systems at harmonic distortions of mains supply voltage // 2015 Intl Aegean Conference on Electrical Machines & Power Electronics (ACEMP), 2015 Intl Conference on Optimization of Electrical & Electronic Equipment (OPTIM) & 2015 Intl Symposium on Advanced Electromechanical Motion Systems (ELECTROMOTION). 2015. doi: 10.1109/optim.2015.7426958
34. Improvement of compensation method for non-active current components at mains supply voltage unbalance / Al-Mashakbeh A. S., Zagirnyak M., Maliakova M., Kalinov A. // Eastern-European Journal of Enterprise Technologies. 2017. Vol. 1, Issue 8 (85). P. 41–49. doi: 10.15587/1729-4061.2017.87316
35. Zagirnyak M., Maliakova M., Kalinov A. Compensation of higher current harmonics at harmonic distortions of mains supply voltage // 2015 16th International Conference on Computational Problems of Electrical Engineering (CPEE). 2015. doi: 10.1109/cpee.2015.7333388
36. Zagirnyak M., Kalinov A., Maliakova M. An algorithm for electric circuits calculation based on instantaneous power component balance // Przegląd elektrotechniczny (Electrical Review). 2011. Issue 12b. P. 212–215. URL: <http://pe.org.pl/articles/2011/12b/59.pdf>
37. Al-Mashakbeh A. S. O. Modern control design of power system // Australian journal of basic and applied sciences. 2009. Vol. 3, Issue 4. P. 4267–4271. URL: https://www.researchgate.net/publication/294390623_Modern_control_design_of_power_system

Розглянуто модель взаємозв'язку основних показників динаміки і надійності з врахуванням конструктивних елементів охолоджуючого пристрою для різних режимів роботи. Одержані співвідношення дозволяють визначити час виходу термоелектричного охолоджуючого пристрою на стаціонарний режим і температуру теплопоглинаючого снаю. Показано, що врахування теплофізичних, конструктивних і енергетичних показників дозволяє управляти часом виходу охолоджувача в стаціонарний режим

Ключові слова: термоелектричний охолоджувач, стаціонарний режим, температура тепло поглинаючого снаю, показники надійності

Рассмотрена модель взаимосвязи основных показателей динамики и надежности с учетом конструктивных элементов охлаждающего устройства для различных режимов работы. Полученные соотношения позволяют определить время выхода термоэлектрического охлаждающего устройства на стационарный режим и температуру теплопоглощающего сная. Показано, что учет теплофизических, конструктивных и энергетических показателей позволяет управлять временем выхода охладителя в стационарный режим

Ключевые слова: термоэлектрический охладитель, стационарный режим, температура теплопоглощающего сная, показатели надежности

UDC 621.362.192

DOI: 10.15587/1729-4061.2018.123891

ANALYSIS OF RELATIONSHIP BETWEEN THE DYNAMICS OF A THERMOELECTRIC COOLER AND ITS DESIGN AND MODES OF OPERATION

V. Zaykov

PhD, Head of Sector
Research Institute «STORM»
Tereshkova str., 27, Odessa, Ukraine, 65076
E-mail: gradan@i.ua

V. Mescheryakov

Doctor of Technical Sciences,
Professor, Head of Department
Department of Informatics
Odessa State Environmental University
Lvivska str., 15, Odessa, Ukraine, 65016
E-mail: gradan@ua.fm

Yu. Zhuravlov

PhD, Associate Professor
Department of Technology of Materials and Ship Repair
National University «Odessa Maritime Academy»
Didrikhsona str., 8, Odessa, Ukraine, 65029
E-mail: zhuravlov.y@ya.ru

1. Introduction

Determining the time that it takes for a thermoelectric cooling device (TED) to enter a stationary working mode

over the preset temperature range is an interesting task. This is related to the fact that dynamic indicators for the means that enable heat regimes of thermally loaded elements largely define both functional and reliable capabilities of critical

systems. In this case, only the mass and specific heat of an object are typically accounted for in the process of entering the mode. At the same time, experience has shown that there is a need to additionally take into consideration the heat capacity and mass of structural and technological elements, as well as current operating mode. In terms of operational control, of special interest is the current mode, and in terms of strategic control – the effect of heat capacity on the dynamic characteristics of a thermoelectric cooling device.

Thus, it is a relevant task to create a controllable dynamic system to monitor temperature at a thermally loaded element.

2. Literature review and problem statement

The issues of enabling thermal modes are integral part of the development of radio electronic equipment whose elements operate under thermally loaded modes [1]. Comparative analysis of compression and solid-state coolers [2] reveals that in terms of weight and dimensions, performance and reliability, thermoelectric coolers have a clear advantage [3]. Improved reliability indicators when designing thermoelectric coolers are achieved by taking into consideration the influence of thermal-physical, electrical properties, chemical activity of the thermoelements' materials when interacting with external environment [4]. Creation of new materials with enhanced thermoelectric efficiency [5] gives rise to new challenges associated with the growing influence of contact resistances, heat conductivity of thermal elements, linear expansion of thermoelement contact with electrode. Specification of requirements to thermoelectric coolers for cooling capacity, energy indicators, weight and dimensions, resulted in the variety of thermoelectric modules [6]. Since such an integrated indicator as reliability depends on the design and manufacturing technology, there are developed methods to investigate indicators of reliability over the entire life cycle, starting at the design stage all the way to operation of thermoelectric coolers [7]. For the on-board systems, the most important is the influence of mechanical and thermal loads. The effect of impact and harmonic mechanical load on the cooler is strengthened by the fact that lower temperatures lead to the worsening of plasticity of the thermoelement soldering with the electrode, and to the increased fragility of a thermoelectric material [8]. Heat load increases temperature gradients, which can lead to the cracking of places where dissimilar materials are connected [9].

Under the non-stationary heat flows, control over coolers for deviation is ineffective. Working out a temperature deviation at the receiving element starts only after the temperature wave reaches the sensor of a thermal control system [10]. Working out a thermal perturbation by the cooler, which is typically described by integrating link, includes the lag time in the process of transition into a stationary mode, during which temperature of the thermally loaded element may exceed maximum permissible temperature. Proactive control implies launching a cooler prior to the moment when the heat wave reaches the cooler, therefore, it employs more complex algorithms to process data in order to make appropriate decisions [11]. The dynamics of control is directly dependent on the performance efficiency of the controlling element, which, in this case, is the cooler [12]. Studies into the inertia of single-stage thermoelectric devices have shown that it is mainly determined by the ratio of heat capacities of the load and a thermoelectric cooler [13]. At the same time, the model considered does not take into

consideration structural and technological elements of the cooler, which are a necessary component of the single-stage thermoelectric cooler. The need to improve performance efficiency of the thermoelectric cooler is in contradiction with the reliability indicators, which requires additional research.

3. The aim and objectives of the study

The aim of present study is to reduce the time it takes for a thermoelectric cooler to enter a stationary regime by taking into consideration the impact of structural and technological elements of the cooler, as well as operational modes.

To accomplish the aim, the following tasks have been set:

- to develop a dynamic model of TED that would account for the structural and technological elements of the cooler;
- to perform a reliability-oriented analysis of the model in order to estimate a possibility to control the time it takes for TED to enter a stationary regime.

4. Development of dynamic model of TED taking into consideration its structural and technological elements

The structural and technological elements on the heat absorbing junction of TED include:

- copper switching plates;
- a layer of soldering and a nickel coating;
- ceramic plate and a metallization layer in line with the switching circuit of thermoelements branches;
- a diffusion layer of a semiconductor material.

The following has to be taken into consideration:

- condition of the thermoelectric material surface, which is related to the technology of processing and storage conditions [8, 9];
- the depth of copper atoms migration in a thermoelectric material.

The thickness of a diffusion layer of the thermoelectric material, a contact area “metal-semiconductor” can be adopted equal to 100–150 μm . We used an aluminum plate with a mass of 1 gram as the object to be cooled. Indicative data on mass and heat capacity of structural and technological elements of TED are given in Table 1. When calculating the volume, for the geometry of thermoelements $l/S = 10 \text{ cm}^{-1}$, we used dimensions of the branch cross-section equal to 2×2 mm at height $l=4 \text{ mm}$.

The total magnitude of heat capacity and the mass of TED components can be represented in the form:

$$\sum_i m_i C_i = m_b C_b + m_{\text{Ni}} C_{\text{Ni}} + m_s C_s + m_{\text{Cu}} C_{\text{Cu}} + m_{\text{cer}} C_{\text{cer}} = 175 \cdot 15^{-4} \text{ J/K}. \quad (1)$$

We shall consider the process of cooling an object in time τ , which is determined by the current mode selected, the magnitude of thermal load Q_0 , branch geometry of the cooling thermoelement (l/S), taking into consideration the temperature dependence of parameters of a thermoelectric material in the module (Fig. 1), as well as specific heat capacity C and thermal diffusivity a (Fig. 2). The dependence of total heat capacity and the mass of structural elements on the geometry of TED branches (l/S) is shown in Fig. 3. The temperature of heat emitting junctions is accepted to be constant and equal to $T=300 \text{ K}$ due to intensive heat exchange.

Table 1

Parameters and indicators of structural and technological elements of the cooler

Elements of design and technology	Width δ , mm	Volume V , cm ³	Density of material ρ , g/cm ³	Mass m , g	Specific heat capacity, C_p , J/(g·K)	mC , J/K	Note
Thermoelectric material Bi ₂ Te ₃	0.1	$2 \times 2 \times 0.1 \cdot 10^{-3} = 4 \cdot 10^{-4}$	7.8	$31.2 \cdot 10^{-4}$	0.31	$19.3 \cdot 10^{-4}$	$m_b C_b$
Antidiffusion nickel-based coating	0.025	$2 \times 2 \times 0.025 \cdot 10^{-3} = 1 \cdot 10^{-4}$	8.1	$8.1 \cdot 10^{-4}$	0.427	$13.8 \cdot 10^{-4}$	$m_{Ni} C_{Ni}$
Solder	0.1	$2 \times 2 \times 0.1 \cdot 10^{-3} = 4 \cdot 10^{-4}$	9.6	$38.4 \cdot 10^{-4}$	0.126	$9.7 \cdot 10^{-4}$	$m_s C_s$
Switching plate, copper	0.2	$2 \times 2 \times 0.2 \cdot 10^{-3} = 8 \cdot 10^{-4}$	9.0	$72 \cdot 10^{-4}$	0.389	$58 \cdot 10^{-4}$	$m_{Cu} C_{Cu}$
Ceramic plate	0.3	$2 \times 2 \times 0.3 \cdot 10^{-3} = 12 \cdot 10^{-4}$	1.84	$22 \cdot 10^{-4}$	1.674	$73.7 \cdot 10^{-4}$	$m_{cer} C_{cer}$
Object to be cooled (Al)	–	–	2.7	1	0.894	0.894	$m_0 C_0$

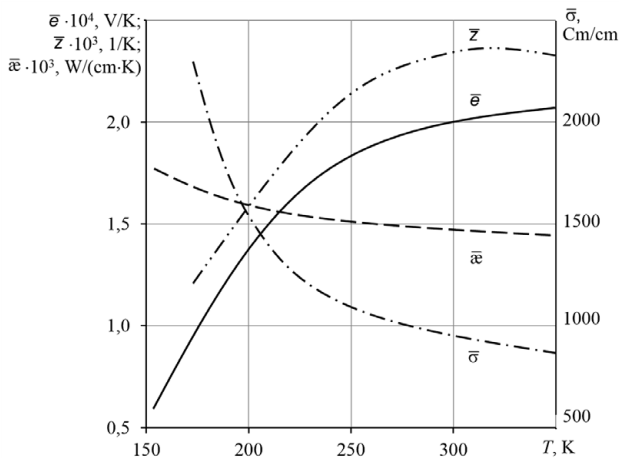


Fig. 1. Estimation-experimental temperature dependence of parameters of thermoelectric materials of the thermoelement branches in module: coefficient of thermoEMF \bar{e} , efficiency of thermoelectric material \bar{z} , coefficient of thermal conductivity \bar{a} and electrical conductivity $\bar{\sigma}$

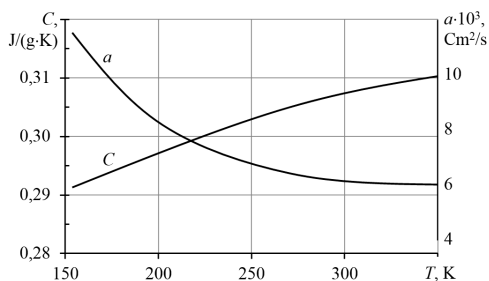


Fig. 2. Estimation-experimental temperature dependence of specific heat capacity C and thermal diffusivity a of the thermoelement branches material in module

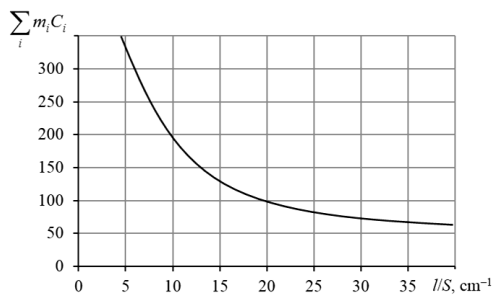


Fig. 3. Dependence of the total magnitude of mass and specific heat capacity of TED structural and technological elements on ratio l/S

Thermal balance conditions on the heat emitting junctions of TED can be written in the form

$$-\left(m_0 C_0 + n \sum_i m_i C_i\right) dT_0 = n I_{\max}^2 R (2B - B^2 - \Theta) d\tau, \quad (2)$$

where m_0, C_0 are, respectively, the mass and specific heat capacity of the cooled object; $I_{\max} = \frac{\bar{e} T_0}{R}$ is the maximum operating current, A; \bar{e}, R are, respectively, the averaged value of coefficient of thermoEMF, V/K, and electrical resistance of the thermoelement branch, Ohm; $B = I/I_{\max}$ is the relative operating current; I is the working current magnitude, A; T_0 is the temperature of a heat absorbing junction, K; $\Theta = \Delta T/T_{\max}$ is the relative difference in temperature; $\Delta T_{\max} = 0.5 \bar{z} T_0^2$ is the maximum temperature difference, K; \bar{z} is the averaged value of the efficiency of a thermoelectric material in module 1/K; $\Delta T = T - T_0$ is the difference in temperature at TED, K; n is the number of thermoelements, pcs.

By solving differential equation (2) under initial conditions $\tau=0; T=T_0$, we shall obtain

$$\tau = \frac{m_0 C_0 + n \sum_i m_i C_i}{n K_1 \left(1 + 2B_1 \frac{\Delta T_{\max}}{T_0}\right)} \ln \frac{\gamma B_1 (2 - B_1)}{2B_2 - B_2^2 - \Theta}, \quad (3)$$

where K_1 is the heat transfer coefficient, $K_1 = \bar{a} S/l$, W/K;

$$\gamma = \frac{I_{\max 0}^2 R_0}{I_{\max 1}^2 R_1};$$

$I_{\max 0}, R_0$ are, respectively, the maximum operating current and electrical resistance of the thermoelement branch at the beginning of the cooling process at $\tau=0$; $I_{\max 1}, R_1$ are, respectively, the maximum operating current and electrical resistance of the thermoelement branch at the end of the process of cooling; \bar{a} is the coefficient of thermal conductivity.

This formula represents an analytical dependence of the time required to enter a stationary mode on the current operating mode (the magnitude of relative current B), heat load Q_0 (number of thermoelements n), taking into consideration both the mass and the heat capacity of the cooled object $m_0 C_0$, and the structural and technological elements of TED at a preset temperature difference $\Delta T(\Theta)$.

Given that $B_1 = I/I_{\max 0}; B_2 = I/I_{\max 1}$, we shall write:

– for mode $Q_{0\max}$

$$I = I_{\max 1}, B_1 = I_{\max 1}/I_{\max 0}, B_2 = 1.0; \quad (4)$$

– for mode $(Q_0/I)_{\max}$:

$$I = \sqrt{\Theta} I_{\max 1}; B_1 = \sqrt{\Theta} I_{\max 1} / I_{\max 0}; B_2 = \sqrt{\Theta}; \quad (5)$$

– for mode E_{\max}

$$I = \Theta I_{\max 1}; B_1 = \Theta I_{\max 1} / I_{\max 0}; B_2 = \Theta; \quad (6)$$

– for mode λ_{\min}

$$I = \eta \Theta I_{\max 1}; B_1 = \eta \Theta I_{\max 1} / I_{\max 0}; B_2 = \eta \Theta; \quad (7)$$

where η is the correction factor [9].

We can derive from equation (3) the temperature of heat-absorbing junction T_0 depending on the cooling time τ :

$$T_0 = T - \frac{2B_1(2-B_1)\Delta T_{\max} \gamma}{\left(1+2B_2 \frac{\Delta T_{\max}}{T_0}\right)} \left\{ 1 - \exp \left[-\frac{n\tau K_1 \left(2B_2 \frac{\Delta T_{\max}}{T_0} + 1\right)}{m_0 C_0 + n \sum_i m_i C_i} \right] \right\}. \quad (8)$$

Expression (8) describes the relationship for various current operating modes and heat load for the assigned temperature difference, taking into consideration the mass and specific heat capacity of structural and technological elements of TED.

5. Analysis of temporal and reliability indicators of the model for different operation modes of TED

The results of calculation of basic parameters and the time required for TED to enter a stationary mode, parameters of reliability for current modes of operation $Q_{0\max}$, $(Q_0/I)_{\max}$, E_{\max} and λ_{\min} at $T=300$ K; $\Delta T=40$ K; $l/S=10$ cm⁻¹; $m_{Al}=1$ g; $C_{Al}=0.894$ J/(g·K) and $\sum_i m_i C_i = 175 \cdot 10^{-4}$ J/K are given in Table 2. Here τ_0 is the time required to enter a stationary mode, calculated with respect to the mass and heat capacity of the object, τ' – with respect to the mass and heat capacity, of both the object and the elements of TED design.

Table 2

Results of calculation of basic parameters and indicators of reliability for a single-stage TED, obtained at the following original data: $I_{\max}=5.02$ A; $T=300$ K; $T_0=260$ K; $\Delta T=40$ K; $l/S=10$ cm⁻¹; $\Delta T_{\max}=79.8$ K; $\Theta=0.5$; $R=1 \cdot 10^{-2}$ Ohm; material Al; $C_{Al}=0.894$ J/(g·K); $m_{Al}=1$ g; $\sum_i m_i C_i = 175 \cdot 10^{-4}$ J/K – per a thermoelement

Mode of operation	Q_0 , A	n , pcs.	τ_0 , s	τ' , W	B_1/B_2	I , A	W , W	E	U , V	λ/λ_0	$\lambda \cdot 10^8$, 1/h	P
$Q_{0\max}$	0.3	2.3	137	143.5	0.93/1.0	5.02	1.39	0.216	0.274	2.35	7.05	0.99930
	0.5	3.9	90.0	96.8			2.30	0.216	0.46	4.0	12.0	0.9988
	1.0	7.8	45.0	51.8			4.53	0.216	0.903	8.0	24.0	0.9976
	1.5	11.7	30.0	36.8			6.83	0.216	1.37	12.0	36.0	0.9964
	2.0	15.6	22.4	29.4			9.10	0.216	1.81	16.0	48.0	0.9952
	3.0	23.4	15.0	21.9			13.6	0.216	2.71	23.9	71.7	0.9929
	5.0	39.0	9.0	15.9			22.7	0.216	4.52	40	120	0.9881
	10.0	78.0	4.5	11.3			45.4	0.216	9.0	79.7	239.1	0.9764
$(Q_0/I)_{\max}$	0.3	2.8	144	152.3	0.66/0.707	3.55	0.88	0.34	0.25	0.73	2.19	0.99978
	0.5	4.7	86.7	94.7			1.44	0.347	0.41	1.23	3.68	0.99963
	1.0	9.4	43.4	51.3			2.88	0.347	0.81	2.45	7.36	0.99926
	1.5	14.1	28.9	36.9			4.40	0.347	1.23	3.68	11.0	0.9989
	2.0	18.8	21.7	29.6			5.88	0.347	1.66	4.9	14.7	0.9985
	3.0	28.2	14.4	22.3			8.80	0.347	2.46	7.35	22.0	0.9978
	5.0	47.0	8.6	16.7			14.7	0.347	4.1	12.3	36.8	0.9963
	10.0	94.0	4.3	12.2			28.8	0.347	8.1	24.5	73.5	0.9926
E_{\max}	0.5	6.6	77.3	87.2	0.47/0.50	2.76	1.10	0.460	0.40	0.607	1.82	0.00081
	1.0	13.0	38.6	48.6			2.20	0.460	0.80	1.20	3.6	0.99964
	1.5	19.5	25.7	35.7			3.30	0.460	1.20	1.82	5.46	0.99946
	2.0	26.0	19.3	29.3			4.40	0.460	1.60	2.42	7.26	0.99928
	3.0	39.0	12.9	22.8			6.60	0.460	2.40	3.64	10.9	0.9989
	5.0	65.0	7.7	17.7			11.0	0.460	4.0	6.0	18.0	0.9982
	10.0	130	3.9	13.8			22.0	0.460	8.0	12.0	36.0	0.9964
λ_{\min}	0.3	6.9	101	114.3	0.40/0.425	2.13	0.88	0.347	0.41	0.215	0.64	0.999936
	0.5	11.6	61.3	75.0			1.40	0.347	0.68	0.361	1.08	0.999892
	1.0	23.2	30.6	44.4			2.88	0.347	1.36	0.722	2.17	0.999780
	1.5	34.8	20.4	34.3			4.32	0.347	2.03	1.07	3.22	0.99968
	2.0	46.4	15.3	29.2			5.76	0.347	2.70	1.43	4.33	0.99957
	3.0	69.6	10.2	24.0			8.64	0.347	4.06	2.16	6.48	0.99935
	5.0	116	6.1	20.0			14.4	0.347	6.80	3.61	10.8	0.9989
	10.0	232	3.0	17.0			28.8	0.347	13.5	7.22	21.7	0.99783

Data in Fig. 4–7 show that an increase in heat load Q_0 (the number of thermoelements n in TED) at the assigned temperature difference ΔT for various current modes of operation leads to the following:

- the time required to enter a stationary mode τ reduces;
- the number of thermoelements n increases;
- voltage drop U grows.

An analysis of data given reveals that the time required to enter a mode τ' increases compared to τ_0 . For example, at thermal load $Q_0=5.0$ W:

- under mode Q_{0max} $\tau_0=9.0$ s; $\tau'=15.9$ s, that is, it is increased by 77 %;
- under mode $(Q_0/I)_{max}$ $\tau_0=8.6$ s; $\tau'=16.7$ s, that is, it is increased by 94 %;
- under mode E_{max} $\tau_0=7.7$ s; $\tau'=17.7$ s, that is, it is increased by 130 %;
- under mode λ_{min} $\tau_0=6.1$ s; $\tau'=20$ s, that is, it is increased by 228 %.

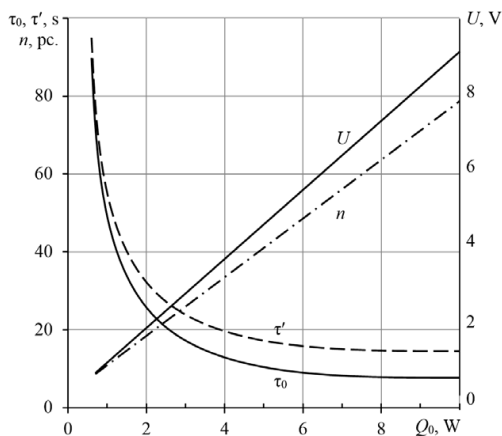


Fig. 4. Dependence of the time required for TED to enter a stationary mode (τ_0 , τ' are, respectively, without and with taking into consideration $\sum_i m_i C_i$), the number of thermoelements n and a voltage drop U of a single-stage TED, on the magnitude of thermal load Q_0 at $T=300$ K; $\Delta T=40$ K; $I/S=10$ cm $^{-1}$ for mode Q_{0max}

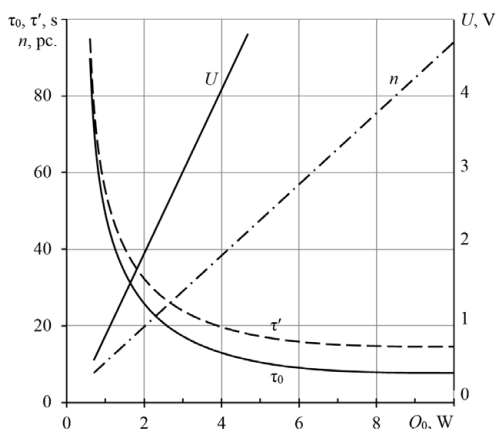


Fig. 5. Dependence of the time required for TED to enter a stationary mode (τ_0 , τ' are, respectively, without and with taking into consideration $\sum_i m_i C_i$), the number of thermoelements n and a voltage drop U of TED, on the magnitude of thermal load Q_0 at $T=300$ K; $\Delta T=40$ K; $I/S=10$ cm $^{-1}$ for mode $(Q_0/I)_{max}$

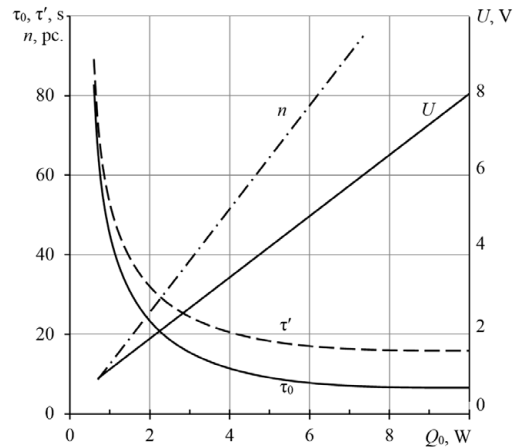


Fig. 6. Dependence of the time required for TED to enter a stationary mode (τ_0 , τ' are, respectively, without and with taking into consideration $\sum_i m_i C_i$), the number of thermoelements n and a voltage drop U of a single-stage TED, on the magnitude of thermal load Q_0 at $T=300$ K; $\Delta T=40$ K; $I/S=10$ cm $^{-1}$ for mode E_{max}

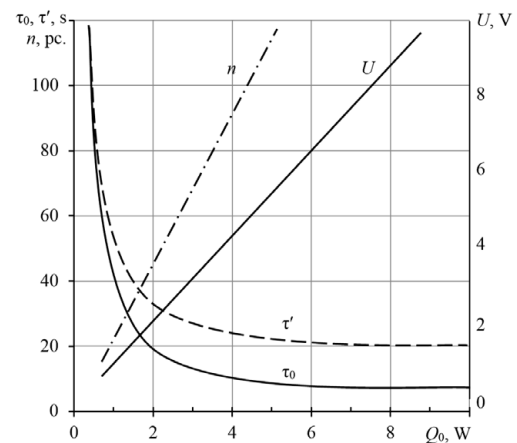


Fig. 7. Dependence of the time required for a single-stage TED to enter a stationary mode (τ_0 , τ' are, respectively, without and with taking into consideration $\sum_i m_i C_i$), the number of thermoelements n and a voltage drop U , on the magnitude of thermal load Q_0 at $T=300$ K; $\Delta T=40$ K; $I/S=10$ cm $^{-1}$ for mode λ_{min}

Fig. 8 shows that the greatest difference between the magnitudes of τ' and τ_0 is observed under a λ_{min} mode.

With a decrease in the time required to enter stationary mode τ , the intensity of failures λ/λ_0 increases for different modes of operation (Fig. 9, a – for modes Q_{0max} and $(Q_0/I)_{max}$, Fig. 9, b – for modes E_{max} and λ_{min}) – due to the increase in the number of thermoelements n in TED.

An analysis of the results of estimating the temporal process of TED entering a stationary mode of operation makes it possible to consider the relation between the mass and heat capacity of the object ($m_0 C_0$) and the mass and heat capacity of structural elements at the heat absorbing junction of TED ($n \sum_i m_i C_i$). The relation can be written in the form:

$$\frac{m_0 C_0}{n \sum_i m_i C_i T_0} = f.$$

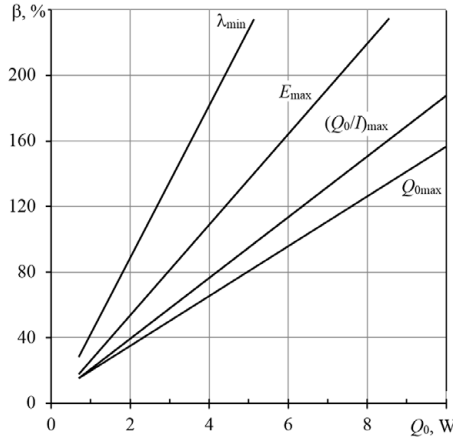


Fig. 8. Dependence of relative magnitude of the time required for a single-stage TED to enter stationary mode $\beta=(\tau'-\tau_0)/\tau_0$ on thermal load at $T=300$ K; $\Delta T=40$ K; $l/S=10$ cm⁻¹ for different modes of operation

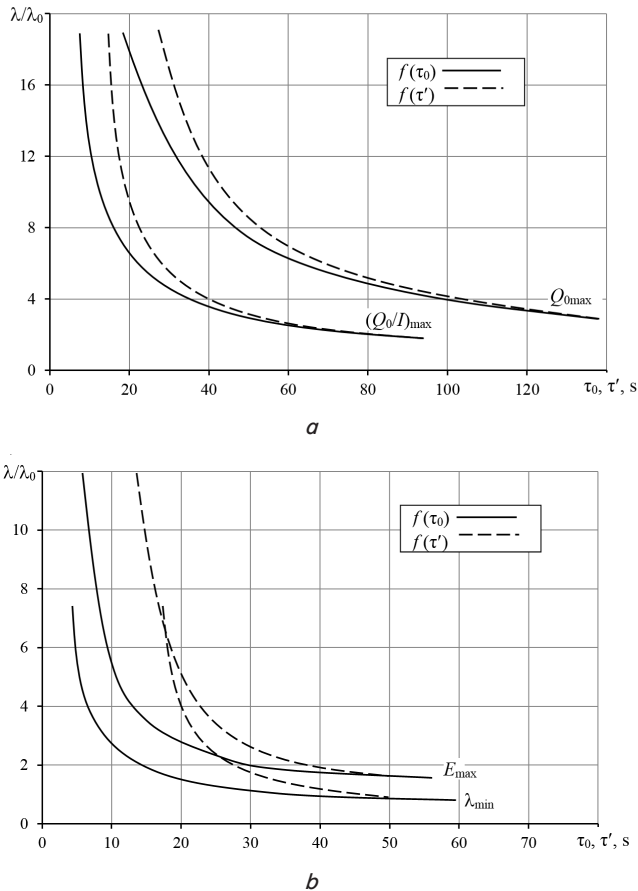


Fig. 9. Dependences of the relative magnitude of failure rate in a single-stage TED on the time required to enter a stationary mode of operation, obtained without and with taking into consideration $\sum_i m_i C_i$, at $T=300$ K; $\Delta T=40$ K; $l/S=10$ cm⁻¹ for different modes of operation: *a* – Q_{0max} , $(Q_0/I)_{max}$; *b* – E_{max} , λ_{min}

A possible range of change in the magnitude *f* can be represented as follows:

a) $f \gg 1$, that is, the mass and heat capacity of the object $m_0 C_0 \gg n \sum_i m_i C_i$ are much larger than the mass and heat

capacity of structural and technological elements of TED. In this case, the relative magnitude of the time required to enter a stationary mode $\tau'/\tau_0 \geq 1.5$. The time required for TED to enter a stationary mode with respect to the mass and heat capacity of structural and technological elements exceeds the time required to enter a stationary mode with respect to the mass and heat capacity of the object by not larger than 50 %;

b) $1.5 \geq f \geq 0.75$, that is, there is an approximate match between the mass and heat capacity of the object, and the mass and heat capacity of structural and technological elements of TED. In this case, the magnitude τ'/τ_0 is in the range of $2.2 \geq \tau'/\tau_0 \geq 1.7$, that is, the time required to enter a stationary mode with respect to the mass and heat capacity of structural and technological elements may exceed the time required to enter a stationary mode without taking them into consideration by the magnitude of 70 to 120 %;

c) $f \ll 1$, that is, the mass and heat capacity of the object are much smaller than the mass and heat capacity of structural and technological elements. In this case, the magnitude $\tau'/\tau_0 \geq 2.2$, that is, the time required to enter a stationary mode with respect to the mass and heat capacity of structural and technological elements is much longer, by 2–10 times, than the time required to enter a stationary mode without taking them into consideration.

Dependence of relative magnitude of the time required for a single-stage TED to enter a stationary mode τ'/τ_0 on the magnitude of *f* at $T=300$ K; $\Delta T=40$ K; $l/S=10$ cm⁻¹ is shown in Fig. 10. It should be noted that a given dependence applies to all the considered modes of operation.

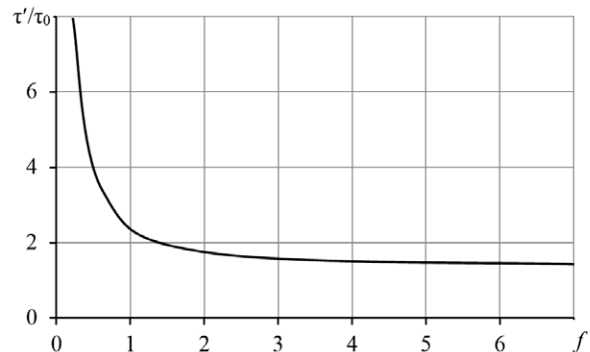


Fig. 10. Dependence of relative magnitude of the time required for a single-stage TED to enter a stationary mode of operation (τ'/τ_0) on the relative magnitude $f = \frac{m_0 C_0}{n \sum_i m_i C_i T_0}$ at $T=300$ K; $\Delta T=40$ K; $l/S=10$ cm⁻¹

In accordance with expression (8), we shall estimate the temperature of a heat-absorbing junction T_0 and other basic parameters for a single-stage TED for the operation modes Q_{0max} , $(Q_0/I)_{max}$, E_{max} and λ_{min} . Initial conditions: $T=300$ K; $\Delta T=40$ K; $l/S=10$ cm⁻¹ with and without taking into consideration the mass and heat capacity of TED structural and technological elements for various thermal load Q_0 . Calculated data are given in Tables 3–6, where T_0 , ΔT_{max} , Θ , λ/λ_0 and P are those without taking into consideration the structural and technological elements; T'_0 , $\Delta T'_{max}$, Θ' , $(\lambda/\lambda)'$ and P' are those taking into consideration the structural and technological elements.

Table 3

Mode Q_{0max} $T=300$ K; $\Delta T=40$ K; $B_1=0.93$; $B_2=1.0$; $I_{max}=5.02$ A; $l/S=10$ cm⁻¹; $C=0.5$ J/(g·K); $m_0C_0=0.894$; $\lambda_0=3 \cdot 10^{-8}$ 1/s; $t=10^4$; $\sum_i m_i C_i = 175 \cdot 10^{-4}$ J/K

Q_0, W	T_0, K	T'_0, K	τ, s	$n, pc.$	ΔT_{max}	$\Delta T'_{max}, K$	Θ	Θ'	λ/λ_0	$\lambda \cdot 10^8, 1/h$	P	$(\lambda/\lambda_0)'$	$\lambda' \cdot 10^8, 1/h$	P'
0,5	293,2	293.6	10	3.9	103,0	103.4	0.068	0.062	2.23	6.7	0.99933	2.21	6.62	0.99934
	287.4	288.2	20		99.1	99.7	0.127	0.118	2.48	7.44	0.99925	2.44	7.33	0.999267
	277.4	278.7	40		92.0	92.8	0.246	0.229	2.96	8.89	0.999111	2.90	8.70	0.99913
	269.4	271.0	60		86.4	87.4	0.354	0.332	3.40	10.2	0.99898	3.32	9.95	0.9990
	263	264.7	80		82.0	83.0	0.451	0.425	3.80	11.4	0.99886	3.70	11.09	0.99889
	260.3	262	90		80	81.0	0.496	0.469	4.0	12.0	0.99880	3.87	11.6	0.99884
	257.8	259.6	95		78.1	79.2	0.54	0.509	4.165	12.5	0.99875	4.04	12.12	0.99879
1.0	287.0	288.6	10	7.8	98.8	100.0	0.132	0.114	5.0	15.0	0.9985	4.86	14.6	0.99854
	276.7	279.2	20		91.9	93.5	0.254	0.222	6.0	18.0	0.9982	5.7	17.2	0.99828
	261.7	265.2	40		80.9	83.0	0.471	0.419	7.76	23.3	0.9977	7.35	22.0	0.9978
	256.6	260.0	50		77.4	79.8	0.56	0.501	8.49	25.5	0.99745	8.0	24.0	0.9976
	259.6	–	44		79.5	–	0.508	–	8.08	24.2	0.99758	–	–	–
1.5	281.6	284.6	10	11.7	94.8	96.8	0.194	0.159	8.26	24.8	0.9975	7.84	23.5	0.99765
	268.5	272.8	20		85.8	88.6	0.367	0.307	10.4	31.1	0.9969	9.65	29.0	0.9971
	261.4	263.9	30		80.6	82.1	0.479	0.44	11.62	34.85	0.99652	11.16	33.47	0.9967
	259.8	–	31		79.6	–	0.504	–	12.05	36.2	0.9964	–	–	–
	–	259.7	36		–	79.6	–	0.506	–	–	–	–	12.1	36.2

Table 4

Mode $(Q_0/l)_{max}$ $T=300$ K; $\Delta T=40$ K; $B_1=0.66$; $B_2=0.707$; $I=3.55$ A; $l/S=10$ cm⁻¹; $C=0.418$ J/(g·K)

Q_0, W	τ, s	T_0, K	T'_0, K	$n, pc.$	ΔT_{max}	$\Delta T'_{max}, K$	Θ	Θ'	λ/λ_0	$\lambda \cdot 10^8, 1/h$	P	$(\lambda/\lambda_0)'$	$\lambda' \cdot 10^8, 1/h$	P'
0.5	10	292.6	293.2	4.7	102.7	103.2	0.072	0.066	0.587	1.76	0.999824	0.579	1.74	0.99983
	20	286	287.1		98.2	98.9	0.143	0.130	0.69	2.07	0.99979	0.672	2.02	0.99980
	40	275.1	276.7		90.4	91.5	0.275	0.255	0.882	2.65	0.99974	0.853	2.56	0.99974
	60	267.9	268.4		85.4	85.7	0.376	0.369	1.04	3.12	0.99969	1.025	3.08	0.99969
	80	259.7	261.8		79.6	80.9	0.506	0.472	1.22	3.67	0.99963	1.175	3.52	0.999648
	85	–	260.4		–	80.0	–	0.495	–	–	–	1.205	3.62	0.99964
1.0	10	286	288	9.4	98.2	99.5	0.143	0.12	1.38	4.14	0.99959	1.32	3.95	0.99950
	20	275.1	278.2		90.4	92.5	0.275	0.236	1.76	5.29	0.99947	1.65	4.96	0.99950
	40	259.7	263.7		78.6	82.4	0.506	0.44	2.44	7.32	0.99927	2.25	6.74	0.99933
	46	–	260.4		–	80.0	–	0.495	–	–	–	2.42	7.25	0.999275
1.5	10	280.2	283.9	14.1	93.8	96.3	0.211	0.167	2.37	7.1	0.99929	2.18	6.54	0.99935
	20	267	271.8		84.8	87.9	0.389	0.321	3.18	9.53	0.99905	2.87	8.6	0.99914
	30	256.9	262.7		77.5	81.8	0.556	0.456	3.94	11.83	0.99882	3.475	10.4	0.99896
	33	–	259.7		–	79.6	–	0.506	–	–	–	3.70	11.1	0.99889

Table 5

Mode E_{max} $T=300$ K; $\Delta T=40$ K; $B_1=0.47$; $B_2=0.50$; $I=2.76$ A; $l/S=10$ cm⁻¹; $C=0.30$ J/(g·K)

Q_0 , W	τ , s	T_0 , K	T'_0 , K	n , pc.	ΔT_{max} , K	$\Delta T'_{max}$, K	Θ	Θ'	λ/λ_0	$\lambda \cdot 10^8$, 1/h	P	$(\lambda/\lambda_0)'$	$\lambda' \cdot 10^8$, 1/h	P'
0.5	10	291.4	292.3	6.5	101.9	102.5	0.084	0.075	0.239	0.718	0.999918	0.232	0.70	0.999930
	20	284.1	285.7		96.9	97.9	0.164	0.146	0.303	0.91	0.999910	0.29	0.87	0.999913
	40	272.5	274.8		88.4	90.0	0.311	0.28	0.429	1.29	0.99987	0.34	1.02	0.999898
	60	264.0	266.5		82.6	84.2	0.436	0.40	0.53	1.59	0.99984	0.50	1.51	0.999849
	70	260.6	–		80.1	–	0.49	–	0.59	1.78	0.99982	–	–	–
	80	–	260.3		–	80.0	–	0.50	–	–	–	0.60	1.79	0.99982
1.0	10	284.1	287	13.0	96.9	98.8	0.164	0.132	0.606	1.82	0.99982	0.556	1.67	0.999833
	20	272.5	276.8		88.4	91.2	0.311	0.254	0.858	2.57	0.99974	0.756	2.27	0.99977
	40	257.7	262.6		78.4	81.4	0.54	0.46	1.27	3.8	0.99962	1.11	3.33	0.99964
	37	259.4	–		79.4	–	0.511	–	1.22	3.66	0.999634	–	–	–
	44	–	259.5		–	79.5	–	0.497	–	–	–	1.19	3.58	0.99964
1.5	10	277.8	283	19.5	91.8	96.1	0.242	0.177	1.105	3.31	0.99967	0.945	2.84	0.99972
	20	264.0	270.8		82.6	87.3	0.436	0.334	1.61	4.84	0.99952	1.34	4.03	0.99960
	25	259.1	–		79.2	–	0.516	–	1.85	5.55	0.999445	–	–	–
	30	–	262.2		–	81.1	–	0.466	–	–	–	1.70	5.1	0.99949
	33	–	260.0		–	79.8	–	0.50	–	–	–	1.80	5.41	0.99946

Table 6

Mode λ_{min} $T=300$ K; $\Delta T=40$ K; $B_1=0.40$; $B_2=0.425$; $I=2.155$ A; $l/S=10$ cm⁻¹; $C=0.17$ J/(g·K)

Q_0 , W	τ , s	T_0 , K	T'_0 , K	n , pc.	ΔT_{max} , K	$\Delta T'_{max}$, K	Θ	Θ'	λ/λ_0	$\lambda \cdot 10^8$, 1/h	P	$(\lambda/\lambda_0)'$	$\lambda' \cdot 10^8$, 1/h	P'
0.5	10	288	290	11.5	99.5	100.9	0.121	0.099	0.123	0.368	0.999963	0.111	0.334	0.999967
	20	278.7	281.9		92.8	95.0	0.23	0.19	0.182	0.546	0.999945	0.16	0.48	0.999952
	40	266.1	270		83.9	86.4	0.404	0.347	0.293	0.878	0.999912	0.255	0.764	0.999924
	60	258.5	262.2		78.9	81.1	0.526	0.466	0.375	1.125	0.999887	0.334	1.0	0.99990
	66	–	260.4		–	80.0	–	0.495	–	–	–	0.355	1.064	0.99989
1.0	10	278.7	284.2	23	92.8	96.9	0.23	0.163	0.364	1.092	0.99989	0.291	0.874	0.999913
	20	266.1	273.1		83.9	88.4	0.404	0.304	0.588	1.76	0.99982	0.457	1.37	0.99986
	30	258.6	265.4		78.9	83.5	0.525	0.414	0.75	2.25	0.999775	0.436	1.31	0.99987
	40	–	260		–	79.8	–	0.50	–	–	–	0.716	2.15	0.999785
1.5	10	271.6	280.5	34.5	88.5	94.0	0.321	0.207	0.721	2.16	0.999784	0.543	1.54	0.99985
	20	258.5	268.2		78.9	85.6	0.526	0.371	1.14	3.41	0.99966	0.814	2.44	0.99976
	29	–	260.5		–	80.0	–	0.494	–	–	–	1.062	3.19	0.99968

Fig. 11–14 show the time-temperature dependences of a heat-absorbing junction T_0 and failure rate λ/λ_0 of a single-stage TED for different modes of operation and varying heat load Q_0 at $T=300$ K; $\Delta T=40$ K; $l/S=10$ cm⁻¹.

Thus, for example, at equal thermal load $Q_0=0.5$ W the time to reach the set temperature of $T_0=260$ K at $T=300$ K and the mass and heat capacity of the object $m_0C_0=0.894$ J/K is:

– under mode Q_{0max} ($B_1=0.93$; $B_2=1.0$; $n=1$): $\tau_0=90$ s; with respect to the mass and heat capacity of TED STE

$\tau'=95$ s, the time required to enter a preset mode increased by 5.5 % at the same failure rate $\lambda/\lambda_0=4$;

– under mode $(Q_0/I)_{max}$ ($B_1=0.66$; $B_2=0.71$; $n=4.7$):

$\tau_0=80$ s, $\tau'=85$ s, the time required to enter a preset mode increased by 6.3 % at $\lambda/\lambda_0=1.22$;

– under mode E_{max} ($B_1=0.47$; $B_2=0.50$; $n=6.5$): $\tau_0=70$ s, $\tau'=80$ s, the time required to enter a preset mode increased by 14 % at $\lambda/\lambda_0=0.6$;

– under mode λ_{min} ($B_1=0.40$; $B_2=0.425$; $n=11.5$): $\tau_0=57$ s, $\tau'=66$ s, the time required to enter a preset mode increased by 14 % at $\lambda/\lambda_0=0.36$.

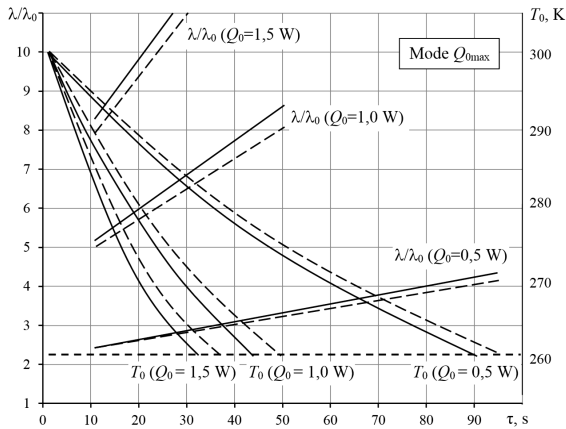


Fig. 11. Time-temperature dependences of a heat-absorbing junction T_0 and failure rate λ/λ_0 for a single-stage TED, obtained without (solid lines) and with (dotted lines) taking into consideration the magnitude of $\sum_i m_i C_i$ at varying heat load Q_0 and $T=300$ K; $\Delta T=40$ K; $l/S=10$ cm⁻¹ for mode Q_{0max}

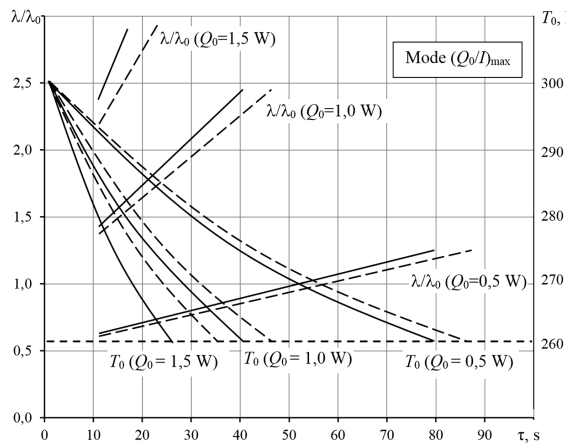


Fig. 12. Time-temperature dependences of a heat-absorbing junction T_0 and failure rate λ/λ_0 for a single-stage TED, obtained without (solid lines) and with (dotted lines) taking into consideration the magnitude of $\sum_i m_i C_i$ at varying heat load Q_0 and $T=300$ K; $\Delta T=40$ K; $l/S=10$ cm⁻¹ for mode $(Q_0/I)_{max}$

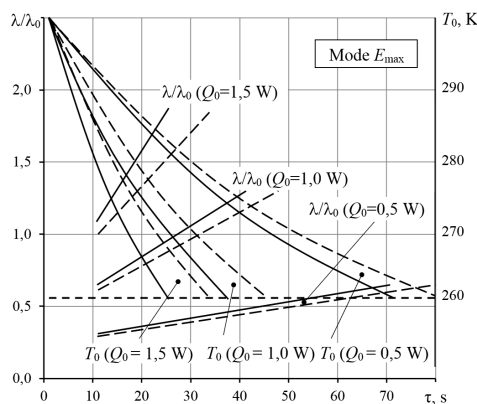


Fig. 13. Time-temperature dependences of a heat-absorbing junction T_0 and failure rate λ/λ_0 for a single-stage TED, obtained without (solid lines) and with (dotted lines) taking into consideration the magnitude of $\sum_i m_i C_i$ at varying heat load Q_0 and $T=300$ K; $\Delta T=40$ K; $l/S=10$ cm⁻¹ for mode E_{max}

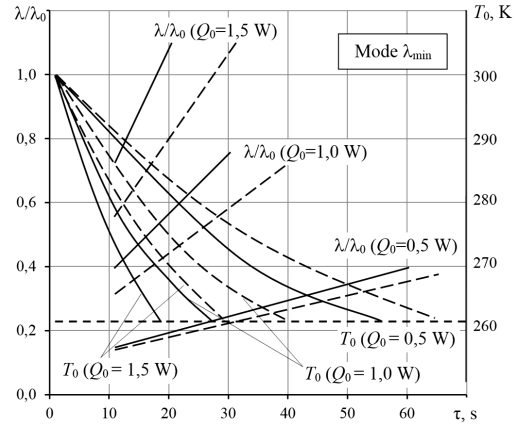


Fig. 14. Time-temperature dependences of a heat-absorbing junction T_0 and failure rate λ/λ_0 for a single-stage TED, obtained without (solid lines) and with (dotted lines) taking into consideration the magnitude of $\sum_i m_i C_i$ at varying heat load Q_0 and $T=300$ K; $\Delta T=40$ K; $l/S=10$ cm⁻¹ for mode λ_{min}

An analysis of the estimation data reveals that the λ_{min} mode ensures minimum time required to enter a stationary mode at minimal failure rate λ/λ_0 for a varying heat load Q_0 .

At a thermal load of $Q_0=1$ W, the time to reach the pre-set temperature $T_0=260$ K at $T=300$ K with a mass and heat capacity of the object of $m_0 C_0=0.894$ J/K is:

- under mode Q_{0max} ($B_1=0.93$; $B_2=1.0$; $n=7.8$): $\tau_0=44$ s; $\tau'=50$ s, that is, the time required to enter a mode increased by 13.6 % at $\lambda/\lambda_0=8$;
- under mode $(Q_0/I)_{max}$ ($B_1=0.66$; $B_2=0.71$; $n=9.4$): $\tau_0=40$ s; $\tau'=46$ s, that is, the time required to enter a mode increased by 15 % at $\lambda/\lambda_0=2.4$;
- under mode E_{max} ($B_1=0.47$; $B_2=0.50$; $n=13$): $\tau_0=37$ s; $\tau'=44$ s, that is, the time required to enter a mode increased by 19 % at $\lambda/\lambda_0=1.2$;
- under mode λ_{min} ($B_1=0.40$; $B_2=0.425$; $n=23$): $\tau_0=29$ s; $\tau'=40$ s, that is, the time required to enter a mode increased by 38 % at $\lambda/\lambda_0=0.72$.

At thermal load $Q_0=1.5$ W, the time to reach the preset temperature of $T_0=260$ K at $T=300$ K, with a mass and heat capacity of the object of $m_0 C_0=0.894$ J/K, is

- under mode Q_{0max} ($B_1=0.93$; $B_2=1.0$; $n=11.7$): $\tau_0=31$ s; $\tau'=36$ s, that is, the time required to enter a mode increased by 16.1 % at $\lambda/\lambda_0=12$;
- under mode $(Q_0/I)_{max}$ ($B_1=0.66$; $B_2=0.71$; $n=14.1$): $\tau_0=26$ s; $\tau'=33$ s, that is, the time required to enter a mode increased by 27 % at $\lambda/\lambda_0=3.8$;
- under mode E_{max} ($B_1=0.47$; $B_2=0.50$; $n=19.5$): $\tau_0=24$ s; $\tau'=32$ s, that is, the time required to enter a mode increased by 33 % at $\lambda/\lambda_0=1.8$;
- under mode λ_{min} ($B_1=0.40$; $B_2=0.425$; $n=34.5$): $\tau_0=19$ s; $\tau'=29$ s, that is, the time required to enter a mode increased by 53 % at $\lambda/\lambda_0=1.1$.

Fig. 15 shows the dependence of relative magnitude of the time required to enter a stationary mode $\beta=(\tau'-\tau_0)/\tau_0$ and relative magnitude of the failure rate λ/λ_0 of a single-stage TED on the magnitude of heat load Q_0 for different modes of operation at $T=300$ K; $\Delta T=40$ K; $l/S=10$ cm⁻¹.

It follows from Fig. 15 that with a growth of thermal load Q_0 for different modes of operation and the preset cooling temperature level $T_0=260$ K and the geometry of thermoelement branches l/S at $T=300$ K:

- the magnitude of relative time required to enter a stationary mode β increases, with the greatest magnitude β observed under the mode of λ_{\min} ;
- the magnitude of relative failure rate λ/λ_0 increases, with the largest magnitude of failure rate λ/λ_0 observed under the mode of $Q_{0\max}$, and the lowest is under the mode of λ_{\min} .

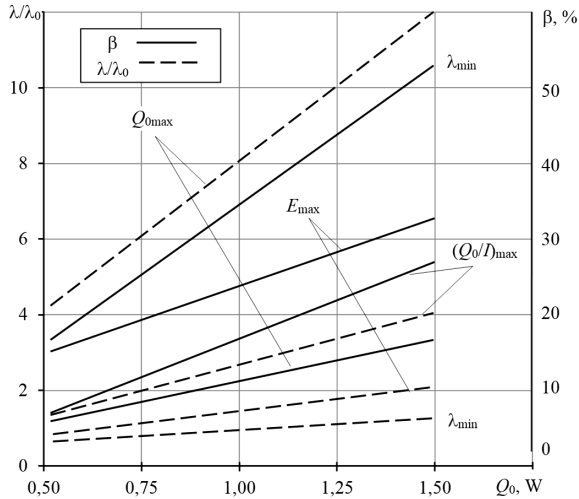


Fig. 15. Dependence of relative magnitudes of the failure rate λ/λ_0 and the time required to enter a stationary mode $\beta=(\tau'-\tau_0)/\tau_0$ of a single-stage TED on thermal load Q_0 at $T=300$ K; $\Delta T=40$ K; $l/S=10$ cm $^{-1}$; $Q_0=0.5$ W; $\lambda_0=3 \times 10^{-8}$ 1/h for different modes of operation

We shall consider a possibility of reducing the time required for a single-stage TED to enter a stationary mode by increasing the number of thermoelements n for a preset heat load Q_0 and temperature difference ΔT : at $T=300$ K; $\Delta T=40$ K; $Q_0=0.5$ W; $l/S=10$ cm $^{-1}$.

Results of the calculations are given in Table 7.

With the increasing number of thermoelements n for a preset heat load Q_0 and temperature difference ΔT (Fig. 16):

- relative operating current B and the magnitude of operating current I decrease;
- voltage drop U grows;
- functional dependence of cooling coefficient $E=f(n)$ has a maximum;
- the time required to enter a stationary mode τ_0 and τ' is reduced; the time required to enter a stationary mode τ' , taking into consideration the structural and technological elements, increases compared to τ_0 : for example, at $n=25$ pcs., $\tau'=61$ s; $\tau_0=41$ s, that is, τ' increases by 53 % (Fig. 17);

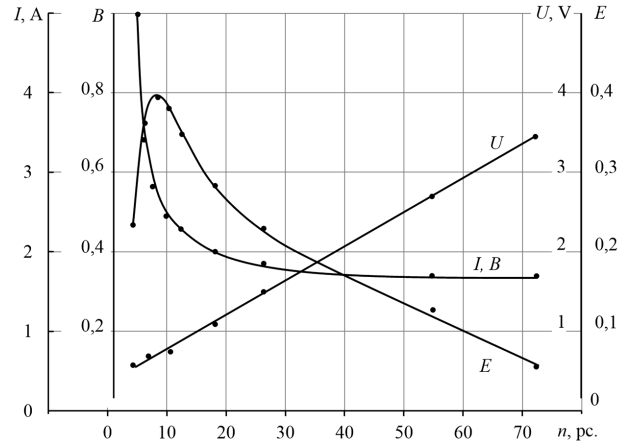


Fig. 16. Dependences of parameters B, I, E, U of a single-stage TED on the number of thermoelements n at $T=300$ K; $\Delta T=40$ K; $l/S=10$ cm $^{-1}$; $Q_0=0.5$ W

- functional dependence of the failure rate $\lambda/\lambda_0=f(n)$ has a minimum at $n_{\lambda_{\min}}$; at $n > n_{\lambda_{\min}}$, failure rate λ/λ_0 increases (Fig. 18);
- relative magnitude of the time required to enter a stationary mode $\beta=(\tau'-\tau_0)/\tau_0$ increases (Fig. 18).

Table 7

$T=300$ K; $T_0=260$ K; $\Delta T=40$ K; $\Theta=0.5$; $I_{\max}=5.02$ A; $R=10.1 \cdot 10^{-2}$ Ohm; $Q_0=0.5$ W

Mode of operation	B_1/B_2	I, A	U, V	E	W, W	$n, pcs.$	τ_0, s	τ', s	$\beta, \%$	λ/λ_0	$\lambda \cdot 10^8, 1/h$	P
$Q_{0\max}$	0.93/1.0	5.02	0.46	0.217	2.30	3.9	83.0	89.5	7.6	4.0	12.0	0.99880
–	0.80/0.86	4.32	0.42	0.275	1.82	4.1	84.9	91.7	8.0	2.345	7.0	0.99930
–	0.72/0.77	3.87	0.41	0.313	1.60	4.4	85.0	92.4	8.7	1.62	4.86	0.99951
I_{\min}	0.66/0.71	3.55	0.411	0.340	1.46	4.7	84.1	91.8	9.1	1.23	3.70	0.99968
–	0.62/0.67	3.38	0.42	0.352	1.42	5.0	83.7	91.9	9.8	1.06	3.19	0.99968
–	0.56/0.60	3.0	0.45	0.374	1.34	5.8	80.4	89.5	11.4	0.765	2.30	0.99977
E_{\max}	0.51/0.55	2.76	0.47	0.385	1.30	6.6	75.4	85.2	12.9	0.61	1.82	0.99982
$(Q_0/I^2)_{\max}$	0.47/0.50	2.51	0.53	0.379	1.32	7.9	72.4	83.5	15.3	0.486	1.46	0.99985
–	0.44/0.47	2.36	0.57	0.372	1.345	9.0	68.7	81.0	18.0	0.428	1.28	0.99987
–	0.39/0.42	2.11	0.70	0.3339	1.475	12.0	60.6	74.8	23.4	0.356	1.07	0.99989
λ_{\min}	0.37/0.40	2.0	0.79	0.316	1.58	14.0	56.3	71.6	27.2	0.330	0.990	0.999901
–	0.35/0.38	1.92	0.92	0.284	1.76	17.0	51.0	67.7	33.0	0.334	1.0	0.999900
L_{\max}	0.32/0.35	1.76	1.30	0.22	2.28	25.3	41.0	61.0	49.5	0.35	1.05	0.999895
–	0.31/0.33	1.66	1.88	0.16	3.13	38.4	31.7	55.5	75.0	0.415	1.245	0.999875
–	0.30/0.32	1.61	2.61	0.12	4.18	54.0	25.0	51.5	106	0.51	1.53	0.99985
–	0.29/0.312	1.57	3.40	0.0936	5.34	72.0	21.0	50.7	141	0.62	1.85	0.99982

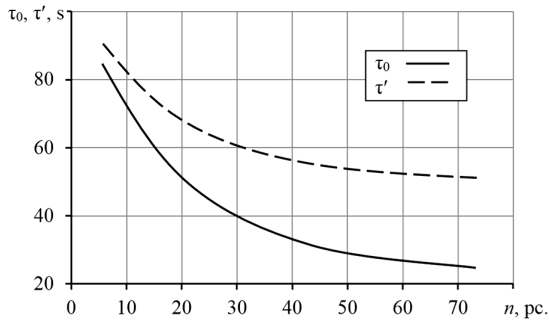


Fig. 17. Dependence of the time required for TED to enter a stationary mode (τ_0, τ' are, respectively, without and with taking into consideration $\sum m_i C_i$) of single-stage TED on the number of thermoelements n at $T=300$ K; $\Delta T=40$ K; $I/S=10$ cm $^{-1}$; $Q_0=0.5$ W

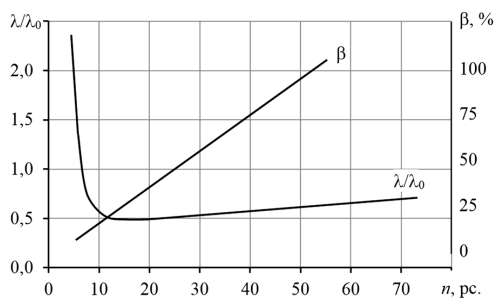


Fig. 18. Dependence of relative magnitudes of failure rate λ/λ_0 and the time required to enter a stationary mode $\beta=(\tau'-\tau_0)/\tau_0$ of a single-stage TED on the number of thermoelements n at $T=300$ K; $\Delta T=40$ K; $I/S=10$ cm $^{-1}$; $Q_0=0.5$ W; $\lambda_0=3 \times 10^{-8}$ 1/h

It should be noted that with an increase in the relative working current B for a preset heat load $Q_0=0.5$ W and a temperature difference $\Delta T=40$ K:

- the magnitude of operating current I increases;
- the magnitudes of voltage drop U and the number of thermoelements n decrease;
- functional dependence of the cooling coefficient $E=f(n)$ has a maximum at current under the mode of E_{max} (Fig. 19);

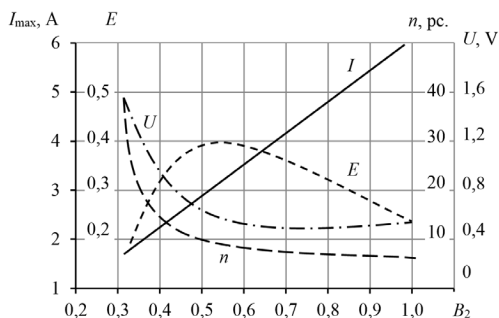


Fig. 19. Dependence of the magnitude of working current I , cooling coefficient E , the number of thermoelements n and voltage drop U of a single-stage TED on the relative working current B_0 for different modes of operation at $T=300$ K; $Q_0=0.5$ W; $\Delta T=40$ K; $I/S=10$ cm $^{-1}$

- failure rate λ/λ_0 grows;
- relative magnitude β decreases (Fig. 20);
- functional dependence of the time required to enter a stationary mode without taking into consideration the

structural and technological elements τ_0 and taking into consideration the structural and technological elements τ' has a flat maximum at $B=0.8$ (Fig. 21).

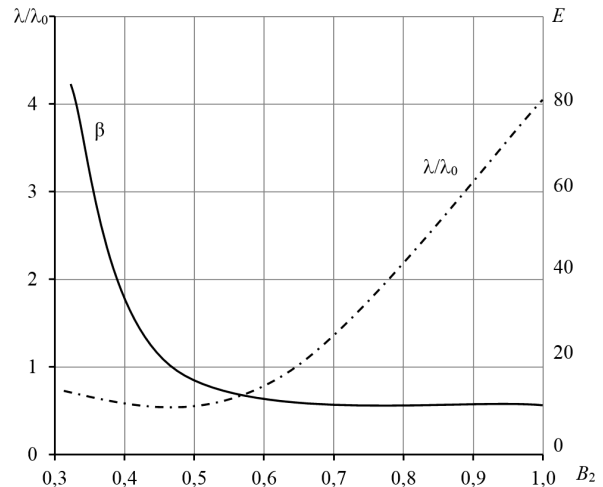


Fig. 20. Dependence of failure rate λ/λ_0 and the magnitude of β for a single-stage TED on relative working current B_2 for different modes of operation at $T=300$ K; $Q_0=0.5$ W; $\Delta T=40$ K; $I/S=10$ cm $^{-1}$

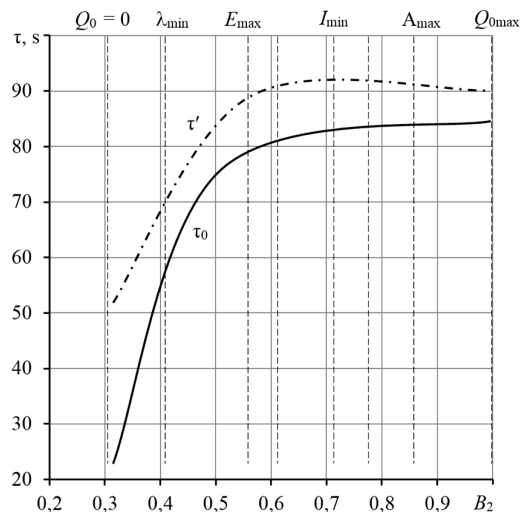


Fig. 21. Dependence of the time required for a single-stage TED to enter a stationary mode τ' and τ_0 on the relative working current B_2 for different modes of operation $T=300$ K; $Q_0=0.5$ W; $\Delta T=40$ K; $I/S=10$ cm $^{-1}$

Thus, it is possible, given the preset value of the time required to enter a stationary mode τ , to determine graphically the magnitude of relative working current B for the assigned temperature difference ΔT and the magnitude of thermal load Q_0 (Fig. 21).

6. Discussion of results of analysis of the time required to enter a stationary mode, energy and reliability indicators of a single-stage TED

The analytical expressions obtained allow us to determine:

- the time required to enter a stationary mode taking into consideration structural and technological elements on

the heat-absorbing junctions of a single-stage TED for different modes of operation $Q_{0\max}$; $(Q_0/I)_{\max}$; E_{\max} ; λ_{\min} , heat load Q_0 and temperature difference $\Delta T=40$ K;

– the temperature of a heat-absorbing junction T_0 depending on time with respect to structural and technological elements for different modes of operation of a single-stage TED and thermal load Q_0 .

An analysis of these expressions shows that if heat capacity and mass of an object are much smaller than the heat capacity and mass of structural and technological elements $f \ll 1$, the time required to enter a mode is much longer than the time required to enter mode τ_0 without taking into consideration these factors.

With an increase in heat load Q_0 :

– the time required to enter stationary mode τ , with respect to the mass and heat capacity of structural and technological elements τ' , and without taking them into consideration τ_0 , is reduced; in both cases, the mass and heat capacity of the cooled object are taken into account;

– voltage drop U and the required number of thermoelements n increase;

– relative magnitude $\beta=(\tau'-\tau_0)/\tau_0$ of the time required to enter a stationary mode grows. The largest gain in the time required to enter a stationary mode is observed under the λ_{\min} mode, the lowest – under the $Q_{0\max}$ mode.

With a decrease in the time required to enter stationary mode τ :

– failure rate λ/λ_0 grows;

– the probability of failure-free operation P for different modes of operation decreases, both with and without taking into consideration the mass and heat capacity of structural and technological elements.

With an increase in the number of thermoelements n at the assigned heat load Q_0 and temperature difference ΔT :

– the time required to enter stationary mode τ_0 and τ' is reduced;

– the relative magnitude of β grows;

– functional dependence of failure rate λ/λ_0 has a minimum at $n=10$ pcs.

With a growth in the relative working current B at a preset temperature difference $\Delta T=40$ K and thermal load Q_0 :

– the magnitude of working current I grows;

– voltage drop U and the number of thermoelements n decrease;

– functional dependence of the cooling coefficient $E=f(B)$ has a maximum at $B=0.55$ (the E_{\max} mode);

– failure rate λ/λ_0 grows, therefore, the probability of failure-free operation P decreases;

– the relative magnitude of β decreases;

– the time required to enter stationary mode τ_0 and τ' increases, both with and without taking into consideration the structural and technological elements.

There is a flat maximum of dependence $\tau=f(B)$ for the E_{\max} mode.

The results obtained could form the basis for the development of control algorithms over dynamic characteristics of single-stage thermoelectric coolers during work with a nonstationary thermal load for the criterion of minimum relative failure rate.

7. Conclusions

1. We have developed an analytical model for the relation between a cooling time of a single-stage thermoelectric cooler with current modes of operation, heat load in the range of working temperature difference, taking into consideration the impact of structural and technological components of the device.

2. The results of analysis of dynamic characteristics, energy and reliability indicators of a single-stage TED showed the possibility to control the time required to enter a stationary mode. Structural control, enabled by selecting the number and geometry of TED thermoelements, and the mass and heat capacity of the load makes it possible to reduce the time required for TED to enter a stationary mode by up to 2.5 times. Operational control, executed by changing working current of the cooler, makes it possible to reduce the time required to enter a stationary mode by up to 3 times.

References

1. Analysis and provision of the thermal characteristics of the radio electronic means' designs using the subsystem ASONIKA-T / Salamova N. A., Shalunov A. S., Martynov O. Yu., Bagaeva T. A. // Successes of modern radio electronics. 2011. Issue 1. P. 42–49.
2. Ndao S., Peles Y., Jensen M. K. Multi-objective thermal design optimization and comparative analysis of electronics cooling technologies // International Journal of Heat and Mass Transfer. 2009. Vol. 52, Issue 19-20. P. 4317–4326. doi: 10.1016/j.ijheatmasstransfer.2009.03.069
3. Perspectives on thermoelectrics: from fundamentals to device applications / Zebarjadi M., Esfarjani K., Dresselhaus M. S., Ren Z. F., Chen G. // Energy Environ. Sci. 2012. Vol. 5, Issue 1. P. 5147–5162. doi: 10.1039/c1ee02497c
4. Materials, Preparation, and Characterization in Thermoelectrics. Vol. 1 / D. M. Rowe (Ed.). 1-st ed. Boca Raton: CRC Press, 2012. 552 p.
5. Sootsman J. R., Chung D. Y., Kanatzidis M. G. New and Old Concepts in Thermoelectric Materials // Angewandte Chemie International Edition. 2009. Vol. 48, Issue 46. P. 8616–8639. doi: 10.1002/anie.200900598
6. Thermoelectric modules market. Analytical review. RosBusinessConsulting, 2009. 92 p.
7. Choi H.-S., Seo W.-S., Choi D.-K. Prediction of reliability on thermoelectric module through accelerated life test and Physics-of-failure // Electronic Materials Letters. 2011. Vol. 7, Issue 3. P. 271–275. doi: 10.1007/s13391-011-0917-x
8. Wereszczak A. A., Wang H. Thermoelectric Mechanical Reliability // 2011 Vehicle Technologies Annual Merit Review and Peer Evaluation Meeting. Arlington, 2011. 18 p.
9. Approach on thermoelectricity reliability of board-level backplane based on the orthogonal experiment design / Zhang L., Wu Z., Xu X., Xu H., Wu Y., Li P., Yang P. // International Journal of Materials and Structural Integrity. 2010. Vol. 4, Issue 2/3/4. P. 170. doi: 10.1504/ijmsi.2010.035205
10. Zaikov V. P., Kinshova L. A., Moiseev V. F. Prediction of reliability on thermoelectric cooling devices. Kn. 1. Single-stage devices. Odessa: Politehperiodika, 2009. 120 p.

11. Egorov V. I. Exact methods for solving heat conduction problems. Sankt-Peterburg: SPb. GU ITMO, 2006. 48 p.
12. Shostakovskiy P. Development of thermoelectric cooling systems and thermostating using the computer program KRYOTHERM // Components and technologies. 2010. Issue 9. P. 113–120.
13. Zaykov V., Mescheryakov V., Zhuravlov Yu. Analysis of the possibility to control of the inertia of the thermoelectric cooler // Eastern-European Journal of Enterprise Technologies. 2017. Vol. 6, Issue 8 (90). P. 17–24. doi: 10.15587/1729-4061.2017.116005

Розглядаються питання обґрунтування вибору конструктивних рішень гідротехнічних водоскидів, робота яких заснована на ефектах контрвихорових течій. Сформульовано підходи до гідравлічного розрахунку проточної частини водоскидів та визначення їх геометричних розмірів. Наводяться основні конструкції локальних завихрювачів, які формують початкові циркуляційно-продовжні течії, даються деякі схеми водоскидних систем з такими завихрювачами потоку

Ключові слова: гідротехнічні скидання води, гашення енергії, закручені потоки, вихрові течії, завихрювач, турбулентність

Рассматриваются вопросы обоснования выбора конструктивных решений гидротехнических водосбросов, работа которых основана на эффектах контрвихревых течений. Сформулированы подходы к гидравлическому расчёту проточной части водосбросов и определению их геометрических размеров. Приводятся основные конструкции локальных завихрителей, которые формируют начальные циркуляционно-продольные течения, даются некоторые схемы водосбросных систем с такими завихрителями потока

Ключевые слова: гидротехнические водосбросы, гашение энергии, закрученные потока, вихревые течения, завихритель, турбулентность

UDC: 532.517.2

DOI: 10.15587/1729-4061.2018.123918

SUBSTANTIATION OF COUNTER-VORTEX SPILLWAY STRUCTURES OF HYDROTECHNICAL FACILITIES

V. Volshanik

Doctor of Technical Sciences, Professor*

E-mail: volshanik@gmail.com

G. Orekhov

Doctor of Technical Sciences,

Associate Professor*

E-mail: orehov_genrih@mail.ru

*Department of Hydraulics and

Hydrotechnical engineering

Moscow State University of Civil

Engineering

Yaroslavskoye highway, 26,

Moscow, Russia, 129337

1. Introduction

The construction and reconstruction of high-pressure waterworks sets a number of scientific and engineering tasks that require a new approach to their solution. One of them is to design reliable and economical culverts, able to work both in the construction and operational periods, making it possible to combine the spillway and energy flow channels. Damping of the excess energy of idle flows is one of the most important tasks when creating hydraulic spillway systems. The choice of the method for damping the kinetic energy of the flow significantly affects the overall layout of the hydraulic engineering structure.

This task becomes the most urgent in the transition to the construction of high-pressure hydraulic systems, which requires studying the phenomena associated with high-speed water flows, their interaction and the development of fundamentally new designs of spillway structures. The hydraulic sections that are used to solve the problems of transit water flows through such structures have been developed. When designing spillways in high-pressure waterworks, it is necessary to take into account the features of the interaction of high-speed flows with solid boundaries and the air environment. It is essential to take into account the probability

of various wave processes, a possible local pressure drop, phenomena of aeration and cavitation and their consequences, as well as peculiarities of energy damping. It is important to ensure ventilation in the case of gravity and partial pressure in closed conduits, as well as take into account other phenomena of hydraulic nature. The resulting hydrodynamic loads under these phenomena are transferred to the building structures, and they must be taken into account in the design, construction and operation of spillway systems.

One of the promising areas for solving these and a number of other problems is the use of swirling water flows in hydrotechnical facilities. The so-called counter-vortex flows of liquid and gas and consideration of the prospects for their practical application have been studied at Moscow State University of Civil Engineering (MGSU, Russia) for several years.

2. Literature review and problem statement

The creation of effective designs of spillway structures for hydrotechnical and hydropower facilities ensures sustainable performance of the entire complex. The design and construction of such systems first and foremost solves the